2014

Evolution of TNF-Induced Apoptosis Reveals 550 My of Functional Conservation

Steven D. Quistad
San Diego State University

Aleksandr Stotland
San Diego State University

Katie Barott
University of Pennsylvania, kbarott@sas.upenn.edu

Cameron A. Smurthwaite
San Diego State University

Brett J. Hilton
San Diego State University

See next page for additional authors

Recommended Citation

Quistad, S. D., Stotland, A., Barott, K., Smurthwaite, C. A., Hilton, B. J., Grasis, J. A., Wolkowicz, R., & Rohwer, F. (2014). Evolution of TNF-Induced Apoptosis Reveals 550 My of Functional Conservation. *PNAS (Proceedings of the National Academy of Sciences), 111* (26), 9567-9572. http://dx.doi.org/10.1073/pnas.1405912111

Evolution of TNF-Induced Apoptosis Reveals 550 My of Functional Conservation

Abstract
The Precambrian explosion led to the rapid appearance of most major animal phyla alive today. It has been argued that the complexity of life has steadily increased since that event. Here we challenge this hypothesis through the characterization of apoptosis in reef-building corals, representatives of some of the earliest animals. Bioinformatic analysis reveals that all of the major components of the death receptor pathway are present in coral with high-predicted structural conservation with *Homo sapiens*. The TNF receptor-ligand superfamilies (TNFRSF/TNFSF) are central mediators of the death receptor pathway, and the predicted proteome of *Acropora digitifera* contains more putative coral TNFRSF members than any organism described thus far, including humans. This high abundance of TNFRSF members, as well as the predicted structural conservation of other death receptor signaling proteins, led us to wonder what would happen if corals were exposed to a member of the human TNFSF (HuTNFα). HuTNFα was found to bind directly to coral cells, increase caspase activity, cause apoptotic blebbing and cell death, and finally induce coral bleaching. Next, immortalized human T cells (Jurkats) expressing a functional death receptor pathway (WT) and a corresponding Fas-associated death domain protein (FADD) KO cell line were exposed to a coral TNFSF member (AdTNF1) identified and purified here. AdTNF1 treatment resulted in significantly higher cell death ($P < 0.0001$) in WT Jurkats compared with the corresponding FADD KO, demonstrating that coral AdTNF1 activates the *H. sapiens* death receptor pathway. Taken together, these data show remarkable conservation of the TNF-induced apoptotic response representing 550 My of functional conservation.

Keywords
evolution immunity, cytokines, Cnidarians, climate change, invertebrate

Disciplines
Biology | Ecology and Evolutionary Biology | Marine Biology | Microbiology

Author(s)
Steven D. Quistad, Aleksandr Stotland, Katie Barott, Cameron A. Smurthwaite, Brett J. Hilton, Juris A. Grasis, Roland Wolkowicz, and Forest Rohwer

Evolution of TNF-induced apoptosis reveals 550 My of functional conservation

Steven D. Quistad[a,1], Aleksandr Stotland[a,b], Katie L. Barott[a,c], Cameron A. Smurthwaite[a], Brett Jameson Hilton[a], Juris A. Grasis[a], Roland Wolkowicz[a], and Forest L. Rohwer[a]

[a]Department of Biology, San Diego State University, San Diego, CA 92182; [b]The Cedars-Sinai Heart Institute, Los Angeles, CA 90048; and [c]Marine Biology Research Division, Scripps Institution of Oceanography, University of California, San Diego, La Jolla, CA 92093

Edited by Max D. Cooper, Emory University, Atlanta, GA, and approved May 8, 2014 (received for review March 31, 2014)

The Precambrian explosion led to the rapid appearance of most major animal phyla alive today. It has been argued that the complexity of life has steadily increased since that event. Here we challenge this hypothesis through the characterization of apoptosis in reef-building corals, representatives of some of the earliest animals. Bioinformatic analysis reveals that all of the major components of the death receptor pathway are present in coral with high-predicted structural conservation with *Homo sapiens*. The TNF receptor-ligand superfamilies (TNFRSF/TNFSF) are central mediators of the death receptor pathway, and the predicted proteome of *Acropora digitifera* contains more putative coral TNFRSF members than any organism described thus far, including humans. This high abundance of TNFRSF members, as well as the predicted structural conservation of other death receptor signaling proteins, led us to wonder what would happen if corals were exposed to a member of the human TNFSF (HuTNFα). HuTNFα was found to bind directly to coral cells, increase caspase activity, cause apoptotic blebbing and cell death, and finally induce coral bleaching. Next, immortalized human T cells (Jurkats) expressing a functional death receptor pathway (WT) and a corresponding Fas-associated death domain protein (FADD) KO cell line were exposed to a coral TNFSF member (AdTNF1) identified and purified here. AdTNF1 treatment resulted in significantly higher cell death ($P < 0.0001$) in WT Jurkats compared with the corresponding FADD KO, demonstrating that coral AdTNF1 activates the *H. sapiens* death receptor pathway. Taken together, these data show remarkable conservation of the TNF-induced apoptotic response representing 550 My of functional conservation.

evolution immunity | cytokines | Cnidarians | climate change | invertebrate immunity

Discoveries from model organisms have significantly influenced the field of human immunology. For example, the original concept of self vs. nonself recognition was discovered from observations in echinoderms, whereas the discovery of Toll-like receptors in humans stemmed from investigations into the response of insects to pathogens. Despite the impact of these studies, the majority of our understanding of immune function remains based on data from a select few taxa, mainly Chordata, Arthropoda, and Nematoda, which represent only 3 of the 30 extant animal phyla (1). Although these models have provided valuable insight into the molecular basis of immune defense, we are overlooking a significant and potentially informative portion of metazoan biology. With the rise of the genomic revolution, an increasing number of genomes from basal phyla are revealing the evolution of immunity to be a nonlinear process, involving multiple instances of gene gain and loss (2). Therefore, the investigation of nontraditional phyla will provide a deeper understanding of the evolution of immunity, including the potential for the discovery of novel immune reactions.

The phylum Cnidaria diverged from Bilateria 550 Mya and contains more than 10,000 species that range in size from a few millimeters to more than 75 m (3). Their body plan consists of two cell layers, an endoderm and ectoderm, held together by the jelly-like mesoglea (4). Stony corals (Order Scleractinia) are colonial cnidarians and are responsible for supporting the most biologically diverse ecosystem on the planet: the coral reef. Reefs support economically important industries such as fishing and tourism and provide coastal protection to hundreds of millions of people worldwide. Recent global surveys have indicated that 19% of coral reefs have been destroyed, 15% are under imminent risk of collapse, and a further 20% are under long-term threat of collapse (5). Anthropogenic impacts such as overfishing and nutrient runoff have been implicated in increased coral death and bleaching (6). However, although many of the environmental factors leading to coral mortality are well established, the biological mechanisms behind coral death remain poorly understood (7, 8).

One common route of coral death on reefs around the world occurs through a process called coral bleaching. During bleaching, the coral's intracellular symbiotic zooxanthellae are expelled from the host (9). Programmed cell death or apoptosis has been observed during the bleaching process; however the components of the apoptotic pathway have yet to be fully identified and functionally tested (10). In humans, apoptosis can be activated through either intrinsic or extrinsic pathways. The intrinsic pathway is initiated by cell stress, whereas the extrinsic pathway is initiated by death ligand/death receptor interactions. Both pathways converge on the members of the B-cell lymphoma family members (Bcl-2) family, which can ultimately lead to caspase activation and the release of signaling molecules such as cytokines to neighboring cells. This process directly links the

Significance

The TNF receptor-ligand superfamily is a central mediator of apoptosis or programmed cell death. Here we show that TNF-induced apoptosis has been functionally maintained for more than half a billion years of evolution. In response to human TNFα, coral cells underwent the classical stages of apoptosis including cellular blebbing, caspase activation, and eventual cell death. Next, the reciprocal experiment showed that coral TNF kills human cells through direct interaction with the death receptor pathway. In addition, corals were found to possess more putative TNF receptors than any organism previously described, including humans. This work provides important insight into the general evolution of apoptosis and demonstrates remarkable conservation of the TNF apoptotic response.

Author contributions: S.D.Q., A.S., R.W., and F.L.R. designed research; S.D.Q., A.S., K.L.B., C.A.S., and B.J.H. performed research; S.D.Q., A.S., C.A.S., B.J.H., and R.W. contributed new reagents/analytic tools; S.D.Q., A.S., K.L.B., C.A.S., B.J.H., J.A.G., R.W., and F.L.R. analyzed data; and S.D.Q. wrote the paper.

The authors declare no conflict of interest.

This article is a PNAS Direct Submission.

Freely available online through the PNAS open access option.

[1]To whom correspondence should be addressed. E-mail: steven.quistad@gmail.com.

This article contains supporting information online at www.pnas.org/lookup/suppl/doi:10.1073/pnas.1405912111/-/DCSupplemental.

apoptotic pathway with the innate immune system (11). In corals, apoptosis has been observed in response to hyperthermic oxidative stress, disease, and as a postphagocytic removal mechanism of zooxanthellae during the onset of symbiosis (10, 12). The recent *Acropora digitfera* genome suggests that coral possess homologs to the human intrinsic and extrinsic apoptotic pathways (13). Although the activation of the intrinsic apoptotic pathway in corals has been observed in response to environmental stress, the extrinsic pathway has yet to be investigated in this system. Specifically, no work to date has focused on the upstream receptor-ligand families involved with apoptotic signaling and activation.

The TNF receptor-ligand superfamily is a central mediator of the extrinsic apoptotic pathway. It is known to be involved in a variety of chronic human diseases such as multiple sclerosis, rheumatoid arthritis, and type 2 diabetes (14). The TNF ligand superfamily (TNFSF) is characterized by a ligand trimerization interface and TNF receptor binding domain. Members of the TNF receptor superfamily (TNFRSF) are defined by the presence of cysteine-rich domains (CRDs), which are important for receptor oligomerization (15). Crystal structure characterization of TNFRSF–TNFSF interactions have also revealed 50s and 90s loop structures that are important for ligand binding and specificity, respectively (15). On ligand binding, the TNFR-1 recruits TRADD, RIP1, and TRAF2, creating complex I, which dissociates from the receptor. Complex I can then activate either the NF-κB transcription factor (among others), leading to cell survival, or bind to Fas-associated death domain protein (FADD), resulting in caspase recruitment and apoptosis (16, 17).

Phylogenetic analysis indicates a deep evolutionary origin of the TNFSF and TNFRSF that precedes the divergence of vertebrates and invertebrates. The most ancient and well-defined invertebrate TNF ligand-receptor system that has been described to date is that of the fruit fly *Drosophila melangastor* (18). *D. melangastor* posseses just one member of both the TNFRSF/TNFSF, in contrast to humans who have 18 and 29, respectively (19). This difference has led to the widely accepted hypothesis that the TNF ligand-receptor superfamily expanded after the divergence of invertebrates and vertebrates (20, 21).

In this paper, we describe the annotation of 40 members of the TNFRSF and 13 members of the TNFSF in the reef building coral *A. digitifera,* suggesting that key parts of the TNF receptor-ligand superfamily have been lost in *D. melangastor* but maintained in coral (22). Comparison of these coral TNFSF/TNFRSF members to those of *Homo sapiens* reveals high genetic and predicted structural conservation. Exposure of coral to human TNFα (HuTNFα) results in apoptotic cellular blebbing, caspase activation, cell death, and finally coral bleaching. Further, we show that exposure of human T-cell lymphocytes to a coral TNFSF member identified and purified here (AdTNF1) directly activates the death receptor pathway in humans. Taken together, these data demonstrate functional conservation of TNF-induced apoptosis across 550 My of evolution. This work also identifies, to our knowledge, the first ligand-receptor signaling pathway to be directly involved in the activation of bleaching and apoptosis in coral. Because coral bleaching events are expected to increase in frequency with future climate change, improving our understanding of the molecular mechanisms involved is prudent for reef conservation and our understanding of the general evolution of apoptosis (23).

Results

Bioinformatic Analysis of the *A. digitifera* Apoptotic Repertoire Reveals High-Predicted Conservation. To elucidate the complexity of the coral apoptotic repertoire, we used the recently published genome of *A. digitifiera* (13). Thirty-one putative TNF receptor-associated factors (TRAFs) with an average length of 458 amino acids were found to have high conservation with *H. sapiens* TRAF1 within the TRAF family domain. (Fig. S1*A* and Table S1). Twenty putative caspases with an average length of 533 amino acids were found to have high conservation within the α/β fold regions of *H. sapiens* caspase-3, including residues located within the caspase-3 active site (Fig. S1*B* and Table S1). Thirteen members of the TNFSF with an average length of 228 amino acids were found to have high conservation with *H. sapiens* TNFα (HuTNFα) with the TNF ligand superfamily domain (Fig. 1*A* and Table S2). Forty putative members of the TNFRSF with an average length of 508 amino acids were also identified within the genome of *A. digitifera* (Table S3). All AdTNFRs contained a minimum of one 50s TNF-binding loop (ligand binding specificity) and one 90s binding loop (receptor oligimerization). The total number of CRDs ranged from zero to four. Eleven of the putative TNFRSF's proteins contained death domains (AdTNFR1–AdTNFR11), whereas five contained Ig domains (AdTNFR18–AdTNFR22). Structural threading of AdTNF1/AdTNFR1 with two members of the human TNFSF/TNFRSF, CD40L and CD40, respectively, suggests high-predicted homology (Fig. 1 *B* and *C*). Compared with previously published work on members of the TNFRSF, corals contain the most diverse TNFRSF repertoire of any organism described to date, including humans (Table S4). *A. digitifera* also possess other canonical apoptotic proteins including Bcl-2 members (8), inhibitors of apoptosis (4), APAF-1, FADD, and cytochrome *c* (Fig. 1*D*). Fig. S2 shows the phylogenetic relationships between AdTNFs, AdTNFRs, AdCasps, and AdTRAFs and *H. sapiens* homologs.

HuTNFα Causes Apoptosis in *Acropora yongeii*. To investigate whether HuTNFα affects coral protein expression, we used Human Explorer Antibody Arrays (Full Moon Biosystems) and found that HuTNFα led to dynamic changes of unknown coral proteins bound to human antibodies to Bcl-$X_{L,}$ Fas, CD40, and multiple CD-receptors (Figs. S3 and S4). To characterize the cellular response of coral to HuTNFα, we first performed immunohistochemistry to demonstrate that HuTNFα binds directly to coral cells (Fig. 2 *A* and *B*). Next we exposed a 20-μm cultured coral cell to HuTNFα under live confocal microcopy and found evidence of apoptotic blebbing within 10 min of treatment (Fig. 2*C*). Quantification of a second 7-μm cell type extracted from adult coral tissue revealed an increase in the number of visible apoptotic cells after 90 min of HuTNFα exposure (Fig. 2*D*). HuTNFα caused a shift in the percentage of apoptotic cells from ∼15% in the untreated coral cells to ∼75% in the HuTNFα-treated cells (n = 200 cells counted; Fig. 2*E*). HuTNFα exposure was also found to significantly increase ($P < 0.0001$) caspase activity of extracted coral cells relative to a negative control inhibitor (Z-FA-FMK; BD Pharmigen) (Fig. 2*F*). Furthermore, 4 h of HuTNFα exposure resulted in a significant ($P < 0.001$) increase in the total number of dead coral cells (Fig. 2*G*). Taken together, these data support the hypothesis that HuTNFα causes apoptosis in the reef-building coral *A. yongeii*.

HuTNFα Causes Myosin Fragmentation and Results in an Acidic Shift in the Coral Proteome. To further examine the effect of HuTNFα on the coral proteome, protein was extracted from untreated coral and coral exposed to HuTNFα and analyzed with 2D gel electrophoresis and LC-MS. Following 30 min of HuTNFα stimulation, 92 spots were found to be significantly different ($P < 0.05$) between the untreated and HuTNFα gels (Fig. 3*A*), with an observed isoelectric shift toward more acidic proteins (Fig. 3*B*). Mass spectra data were compared with a custom-built coral protein database created from the predicted proteome (13). Four separate spots were identified as coral myosin (adi_v1.18643), which increased on HuTNFα exposure (Fig. 3*A*, spots 2, 3, 5, and 6). The predicted molecular mass of coral myosin is ∼316 kDa, whereas the four identified myosin spots ranged from 70 to 84 kDa, suggesting cleavage. In addition, the banding pattern

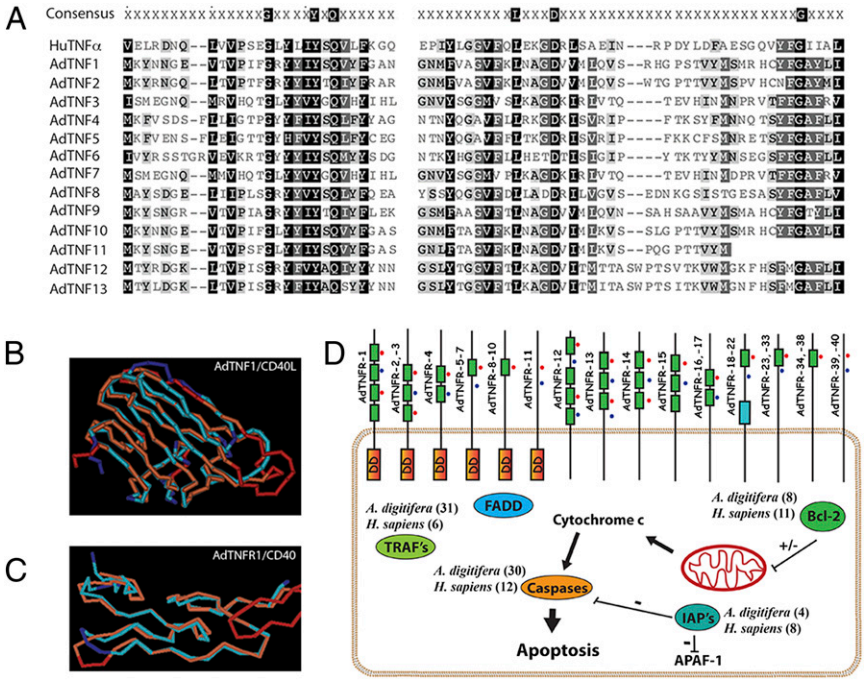

Fig. 1. Bioinformatic analysis of coral and human proteins involved with death receptor signaling. (*A*) Primary sequence alignment of putative *A. digitifera* TNF ligands with *H. sapiens* TNFα. (*B*) Predicted structural alignment of AdTNF1 (residues 25–161) and *H. sapiens* CD40L. Light blue and orange = high predicted structural homology, dark red = CD40L, and dark blue = AdTNF1 (*C*). Predicted structural alignment of AdTNFR1 (residues 19–79) with *H. sapiens* CD40. Light orange and light blue = high-predicted structural homology, dark red = CD40, and dark blue = AdTNFR1. (*D*) The putative TNFR repertoire of *A. digitifera* (*Upper*) with death domain (DD), cysteine-rich domain (green boxes), immunoglobin domain (blue box), 50s loop TNF binding site (red dot), and 90s loop TNF binding site (blue dot) indicated. Members of the death receptor signaling pathway (*Lower*) found in the *A. digitifera* genome with number of proteins within a specific protein family indicated for both *A. digitifera* and *H. sapiens* including TNF receptor associated factors (TRAFs), B-cell lymphoma family members (Bcl-2), inhibitor of apoptosis proteins (IAPs), FADD, APAF-1, and caspases.

observed in Fig. 3*C* is suggestive of myosin phosphorylation. The initial induction of apoptosis also affects calcium signaling (24), and following HuTNFα exposure, two proteins that contain an EF-hand calcium binding site and calreticulin were found to be up-regulated (Table S5), suggesting that HuTNFα affects calcium signaling in corals. Finally the Zooxanthallae-specific protein Peridinin was also up-regulated, providing initial evidence that HuTNFα affects coral-algal symbiosis (Fig. 3*C* and Table S5).

HuTNFα Causes Bleaching of *A. yongeii*. To test whether HuTNFα-induced apoptosis is also involved in coral bleaching, we used a flow cytometric approach. Coral tissue was found to expel zooxanthellae in the presence and absence of treatment with HuTNFα (Fig. S5 *A* and *B*). Untreated coral initially expelled more zooxanthellae after 1 h than HuTNFα-treated coral; however, after 7 h, the HuTNFα-treated coral expelled ∼200% more algae than the untreated coral (Fig. S5*C*). When both untreated and HuTNFα-treated corals were exposed to 100 mg/mL of ampicillin (AMP), the untreated control initially released more zooxanthallae than the HuTNFα-treated coral. However, at 10 h, the +HuTNFα/+AMP-treated coral had ∼400% more expelled algae, which increased to ∼500% by 12 h (Fig. S5*D*). From 6 to 12 h, the zooxanthellae released by the −HuTNFα/+AMP coral remained relatively constant at ∼2,000 expelled algal cells (Fig. S5*D*).

Crude AdTNF1 Causes Apoptosis in Coral and Is Involved with Bleaching. To conduct preliminary investigations into the biological effects of one of the newly described coral TNF ligands (AdTNF1), we created a construct with a Prolactin signal sequence fused to AdTNF1 ensuring its secretion into the surrounding media (PBMN.i.mChAdTNF1) (25). A diagram representing the constructs for the secretion of GFP and AdTNF1 is presented in Fig. S5*A*. As a control, a construct with GFP fused to a Prolactin signal sequence was also created (pBMN.i.mChGFP). 293T cells transfected with pBMN.i.mChGFP displayed stable expression of GFP localized to the endoplasmic reticulum/trans-Golgi, as expected of secreted proteins (Fig. S6*B*). Exposure of coral cells to 10 μL of media from 293T cells transfected with pBMN.i.mChAdGFP control resulted in ∼20% apoptotic cells, whereas cells exposed to media from the pBMN.i.mChAdTNF1 resulted in ∼80% apoptotic cells (n = 200; Fig. S5*C*). Adult coral tissue exposed to 250 μL of pBMN.i.mChAdTNF1 media resulted in a significant ($P < 0.05$) reduction in total algae expelled at 4 h posttreatment; however, there was no significant difference from the control by 6 h (Fig. S6*D*). Finally, the FLAG (26) epitope was cloned into the C terminus of AdTNF1, and evidence for direct binding of AdTNF1-FLAG to coral cells is presented in Fig. S6 *E* and *F*.

Purified Coral AdTNF1 Causes Apoptosis in Human T-Lymphocytes. To directly test whether coral AdTNF1 interacts with the human death receptor pathway, we used WT immortalized human T lymphocytes (Jurkats) and a corresponding FADD KO cell line (ATCC CRL-2572; Fig. 4*A*). AdTNF1 was further purified through His-tag nickel affinity chromatography (Fig. 4*B*; Monserate Biotechnology Group) and used for subsequent experimentation. Bioinformatic analysis demonstrates high-predicted structural conservation between AdTNF1 and FasL (27) (Fig. 4*C*). Propidium iodide staining demonstrated that FasL negatively affects WT cell viability in a dose-dependent manner, whereas FADD KO cell viability is unaffected (Fig. S7*A*). Next we exposed both WT and FADD KO cells to AdTNF1. Following 48 h of AdTNF1 treatment, WT Jurkat cells exhibited a significant ($P < 0.0001$) reduction in cell viability compared with the FADD KO cells,

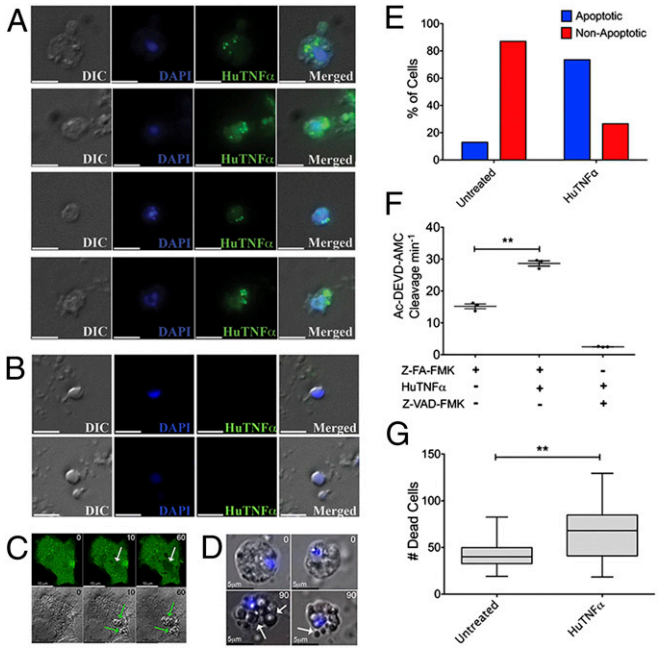

Fig. 2. Effect of HuTNFα on *A. yongeii* cell populations. (*A*) Representative coral cells incubated with HuTNFα and HuTNFα antibody, stained with DAPI. (White bar, 5 μm.) (*B*) Representative coral cells incubated with HuTNFα antibody and stained with DAPI. (White bar, 5 μm.) (*C*) Live confocal microscopy of a GFP autoflourescent coral cell exposed to HuTNFα at 0, 10, and 60 min. (White bar, 10 μm.) White/green arrow indicates regions of apoptotic body formation. (*D*) Representative images of apparently healthy coral cells (*Upper*) and apoptotic cells (*Lower*) stained with DAPI at 0 and 90 min. (Black bar, 5 μm.) White arrows indicate apoptotic bodies. (*E*) Relative percentages of apoptotic/nonapoptotic coral cell populations left untreated or incubated with HuTNFα for 90 min (n = 200 cells). (*F*) Caspase activity of coral cells stimulated with HuTNFα for 30 min with negative control inhibitors (Z-FA-FMK) and pan-caspase inhibitors (Z-VAD-FMK) indicated (**P = 0.0024; unpaired t test with ±SEM indicated). (*G*) Total number of dead cells per image (n = 32 images) under untreated conditions and HuTNFα exposure for 4 h with interquartile ranges (boxes) and whiskers (10–90 percentiles) indicated (**P = 0.0011; unpaired t test).

demonstrating that coral AdTNF1 directly interacts with the death receptor pathway in humans, increasing cell death (Fig. 4*D* and Fig. S7*B*).

Discussion

HuTNFα exposure led to increased caspase activity, cellular blebbing, and cell death, demonstrating that HuTNFα causes apoptosis in coral. Furthermore, AdTNF1 was found to directly interact with the *H. sapiens* death receptor pathway, also resulting in cell death. This suggests that apoptotic signaling through TNFRSF/TNFSF proteins was fully functional at the time of the pre-Cambrian explosion, and remarkably, the domains necessary to activate apoptosis have been maintained from corals to humans.

A recent review by Weins et al. (21) explored the origin and evolution of the TNF receptor-ligand superfamilies and concluded that their evolutionary origin could be traced back to single copy genes within arthropods. They posit that these founding genes underwent multiple duplication events following the divergence of invertebrates and vertebrates, which coincided with the development of the adaptive immune system (21). However, this study failed to take into account the recently published Cnidarian genomes of *Nematostella vectensis* and *A. digitifera* (2, 13). The existence of 40 putative coral TNF receptors (AdTNFR1–AdTNFR40) and 13 putative coral TNF ligands (AdTNF1–AdTNF13) identified here suggests a far more ancient origin of the TNF receptor-ligand superfamily that precedes arthropods. Our data demonstrate high conservation of TNFRSF/TNFSF members in corals, suggesting the last common metazoan ancestor possessed a functional TNF apoptotic pathway, which subsequently underwent gene reduction in arthropods and other invertebrates. Corals possess more putative members of the TNFRSF of any organism described thus far and possess a similar number of putative TNFSF proteins as many vertebrates (Table S5) (21). Although the function of AdTNFR1–AdTNFR40 and AdTNF1–AdTNF13 still requires elucidation, the TNF receptor-ligand superfamily has clearly undergone dynamic changes throughout the various lineages of metazoan evolution, independent of a particular phylum's structural complexity. Similar complexity has also been observed in the Cnidarian *N. vectensis* within the Nme and Wnt gene families, a complexity that has also been lost in other model ecdyzoans (28, 29). These studies, along with ours, highlight the need to take into account the genomes of a broad range of animal phyla before we can draw broad conclusions about the evolution of gene families.

Beyond the specific TNF ligand-receptor pathway, the general existence of cytokines in invertebrates has been argued to be the result of convergent evolution (30–32). For example, in *D. melangastor*, the Toll-like receptor pathway is involved in the response to microbial infection. On immune stimulation, protease cascades lead to the activation of the cytokine Spatzle (33). In humans, the related pathway involves the Toll-like receptor (IL1-R1) and its respective ligand (IL-1) (34). Although both the *D. melangastor* Toll and human IL-1 pathways converge on the activation of NF-κB transcription factor homologs, IL-1 and Spatzle do not show any significant similarity at the amino acid level. Furthermore, the completed genome of *D. melangastor* failed to reveal any proteins homologous to human IL-1. From these data, it was concluded that invertebrates lack any

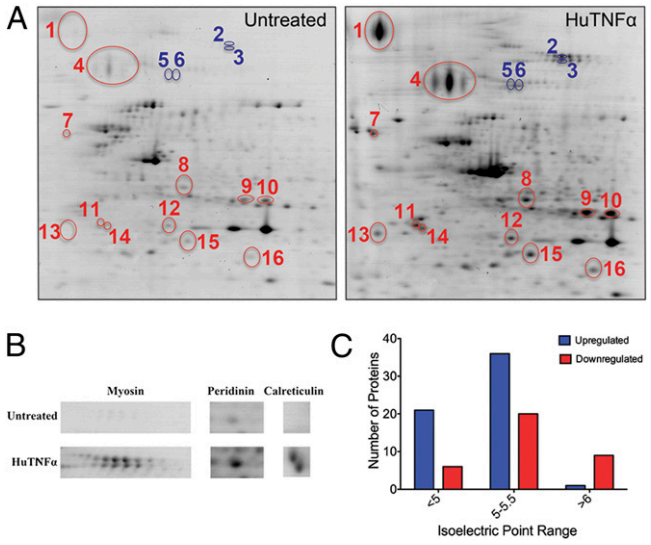

Fig. 3. Proteomic analysis of coral exposed to HuTNFα using 2D gel electrophoresis. (*A*) 2D gel electrophoresis of extracted protein from untreated coral (*Left*) and human TNFα-stimulated coral (*Right*) for 30 min. Numbered circles indicate proteins that were identified through MS, whereas blue circles indicate fragments of myosin. (*B*) Representative proteins that were up-regulated in response to HuTNFα including myosin, the zooxanthallae-specific protein peridinin, and calreticulin. (*C*) Ninety-two proteins that were significantly different between the untreated and human TNFα-treated gels grouped by their respective isoelectric points. Red bar indicate the number of proteins in a specific p*I* range that were down-regulated in response to HuTNFα stimulation. Blue bars represent the number of proteins in a specific p*I* range that were up-regulated in response to HuTNFα stimulation.

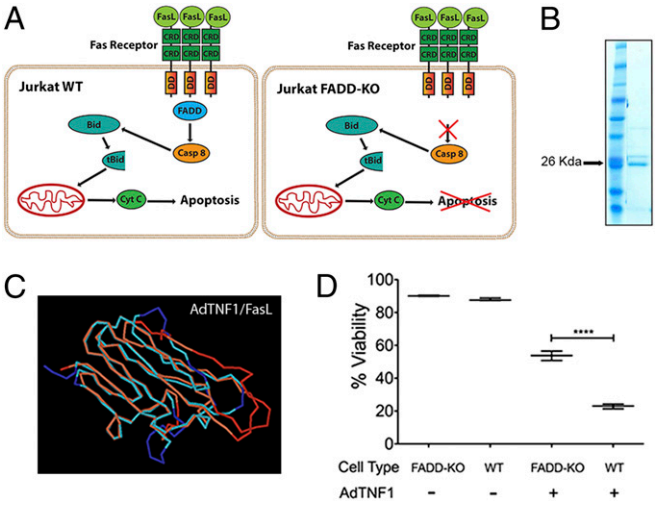

Fig. 4. Effect of AdTNF1 on human T-lymphocyte cellular viability. (*A*) T-cell lymphoma cell lines (Jurkat) used for experimentation. WT cells are sensitive to Fas-induced apoptosis, whereas FADD KO are resistant. (*B*) Production and isolation of His-tagged AdTNF1 through Nickel-affinity chromatography with correct size of His-AdTNF1 indicated. (*C*) Predicted structural alignment of FasL and AdTNF1. Light orange and light blue = high-predicted structural homology, dark red = FasL, and dark blue = AdTNFR1. (*D*) The effect of AdTNF1 on cellular viability of WT and FADD KO Jurkat cell lines (****$P <$ 0.0001; unpaired *t* test).

homologous pathway to vertebrate IL-1/IL-1-R signaling. Beyond the specific IL-1 pathway, multiple vertebrate and invertebrate cytokines have been shown to exhibit similar biological functions, yet they lack any genetic homology (30). It was therefore postulated that the similar biologically activities of these cytokines is a result of convergent evolution. However, the vast majority of data supporting this hypothesis are taken from the model systems of *D. melangastor* and *Caenorhabditis elegans*, which as discussed above have lost complexity in multiple gene networks. The high amino acid conservation between coral TNFRSF members and HuTNFα, as well as the activation of apoptosis in coral using a human cytokine, support the hypothesis of a divergent evolution of the TNF receptor-ligand superfamily. Future work should focus on the cytokine repertoire of other phyla to develop a comprehensive hypothesis of metazoan cytokine evolution.

The canonical apoptotic cascade is executed by a group of cysteine-dependent aspartate-directed proteases known as caspases, which, on activation by the adaptor protein FADD, cleave various cellular substrates, leading to apoptotic body formation and eventual cell death. Within FADD, two essential domains designated the death domain (DD) and death effector domain (DED) are required for apoptotic transduction (35). A putative FADD protein containing the DD and DED domains has been identified in both *Hydra* and the *A. digitifera* proteome (aug_v2a.04795) (36, 37). On activation of apoptosis, the phosphorylation and cleavage of the myosin-light chain are critical for the subsequent morphological changes involved with cellular blebbing (38). Fragments of coral myosin were found to significantly increase on HuTNFα stimulation, and the associated banding pattern in response to HuTNFα is suggestive of a phosphorylation event (Fig. 3*C*). Furthermore, the acidic shift of the 92 proteins could also be the result of a larger phosphorylation cascade (Fig. 3*B*) (39). Interestingly, one of the most highly up-regulated proteins in the HuTNFα-stimulated gel contained a Zona-Pellucida (ZP) domain, which has traditionally been studied within the context of fertilization (40). Although ZP domain proteins have not been well studied within the context of TNF signaling in humans, preexposure of sperm to HuTNFα impairs sperm binding (41). The role of ZP domain proteins in the coral TNF signaling cascade should be a focus of future studies.

Although previous studies have demonstrated apoptotic coral cells in whole coral tissue, to the authors' knowledge, Fig. 2 reveals the first images of an isolated coral cell undergoing cytokine-induced apoptosis (42). We hypothesize that HuTNFα binds to one of the AdTNF receptors containing a death domain (AdTNF1–AdTNF6), initiating the apoptotic cascade and caspase activation (Fig. 2*F*). A biochemical model of bleaching has been proposed in which reactive oxygen species (ROS) production by the algal symbionts compromises the structural integrity of the mitochondrial membrane, stimulating the release of apoptotic factors and caspase activation (43). With the identification of a diverse repertoire of 40 putative TNF receptors and 13 putative TNF ligands described here, as well as the potential involvement of the mitochondria on HuTNFα exposure (Fig. S3*C*), we propose supplementing this model with further investigation into the specific members of the coral TNFRSF/TNFSF and their involvement in bleaching and apoptotic processes.

Previous investigations into the mechanism of coral bleaching have largely relied on thermal stress to induce zooxanthellae expulsion. Although environmentally relevant, the application of thermal stress causes dynamic changes to the coral holobiont making a determination of the specific signaling pathways directly involved in apoptosis and bleaching challenging if not impossible (44). In this study, we induced both of these cellular processes through the application of a single protein to adult coral tissue and individual coral cells. Although previous work has investigated the downstream effectors of apoptosis such as caspases (43) and Bcl-2 family members (42), this is the first examination, to our knowledge, of the upstream ligands and receptors involved with initiating apoptosis in coral. Recently published transcriptomic studies of corals exposed to various environmental stressors have implicated members of the TNFSF/TNFRSF, as well as downstream proteins involved with apoptosis, supporting the ecological relevance of the TNF pathway in coral (45–49).

This study reveals an ancient origin of the TNF receptor-ligand superfamily. The activation of apoptosis in coral using a human TNF ligand (Fig. 2) in conjunction with the induction of apoptosis in humans using coral AdTNF1 (Fig. 4) demonstrates remarkable evolutionary conservation that has been functionally maintained for 550 My. Although we demonstrate that AdTNF1 specifically interacts with the death receptor pathway in humans, the mechanism remains unknown. Furthermore, the existence of 12 additional coral TNF ligands (AdTNF2–AdTNF13) and the interactions of those TNF ligands with human cell physiology create exciting possibilities for future research.

Materials and Methods

Members of the coral TNFSF/TNFRSF were bioinformatically extracted from the *A. digitifera* proteome (13) and analyzed using the DAS transmembrane prediction server (50), PRO-SITE database (51), and the Conserved Domain Database (52). Coral cell culture methods were adapted from Helman et al. (53) and Reyes-Bermudez and Miller (54) and utilized for immunohistochemistry, caspase activity, and live-dead cell assays. AdTNF1 was purified through His-tag nickel affinity chromatography (Monserate Biotechnology Group) and used for subsequent experimentation. Jurkat WT and Jurkat FADD KO cells (ATCC CRL-2572) were exposed to AdTNF1, stained with propidium iodide, and sorted through flow cytometry. See *SI Materials and Methods* for further details.

ACKNOWLEDGMENTS. We thank Leo Su and the Monserate Biotechnology Group for the purification of AdTNF1, Fernando Nosratpour and Vince Levesque at the Birch Aquarium for their generous donation of *A. yongeii*, Phillip Cash (Aberdeen Proteomics) for 2D-Gel analysis, Rob Edwards for array suggestions, Nikki Traylor-Knowles for helpful comments with the manuscript, and the San Diego State University FACS facility. This work was funded by a National Science Foundation Graduate Research fellowship (to S.D.Q.), National Institutes of Health Grant 1 R21 AI094534-01 (to F.L.R.), and the Canadian Institute For Advanced Research Integrated Microbial Diversity Fellowship (IMB-ROHW-141679) (to F.L.R.).

1. Litman GW, Cooper MD (2007) Why study the evolution of immunity? *Nat Immunol* 8(6):547–548.
2. Putnam NH, et al. (2007) Sea anemone genome reveals ancestral eumetazoan gene repertoire and genomic organization. *Science* 317(5834):86–94.
3. Daly M, et al. (2007) The phylum Cnidaria: A review of phylogenetic patterns and diversity 300 years after Linnaeus. *Zootaxa* 1668:127–182.
4. Augustin R, Bosch TCG (2010) Cnidarian immunity: A tale of two barriers. *Adv Exp Med Biol* 708:1–16.
5. Bourne DG, et al. (2009) Microbial disease and the coral holobiont. *Trends Microbiol* 17(12):554–562.
6. Brown BE (1997) Coral bleaching: Causes and consequences. *Coral Reefs* 16-(Suppl):S129–S138.
7. Rosenberg E, Kushmaro A, Kramarsky-Winter E, Banin E, Yossi L (2009) The role of microorganisms in coral bleaching. *ISME J* 3(2):139–146.
8. Lesser M (2011) Coral bleaching: Causes and mechanisms. *Coral Reefs: An Ecosystem in Transition*, eds Dubinsky Z, Stambler N (Springer, Houten, The Netherlands), pp 405–419.
9. Davy SK, Allemand D, Weis VM (2012) Cell biology of cnidarian-dinoflagellate symbiosis. *Microbiol Mol Biol Rev* 76(2):229–261.
10. Dunn SR, Schnitzler CE, Weis VM (2007) Apoptosis and autophagy as mechanisms of dinoflagellate symbiont release during cnidarian bleaching: Every which way you lose. *Proc Biol Sci* 274(1629):3079–3085.
11. Zhou F, Yang Y, Xing D (2011) Bcl-2 and Bcl-xL play important roles in the crosstalk between autophagy and apoptosis. *FEBS J* 278(3):403–413.
12. Weis VM (2008) Cellular mechanisms of Cnidarian bleaching: Stress causes the collapse of symbiosis. *J Exp Biol* 211(Pt 19):3059–3066.
13. Shinzato C, et al. (2011) Using the Acropora digitifera genome to understand coral responses to environmental change. *Nature* 476(7360):320–323.
14. Bahia MS, Silakari O (2010) Tumor necrosis factor alpha converting enzyme: An encouraging target for various inflammatory disorders. *Chem Biol Drug Des* 75(5): 415–443.
15. Hymowitz SG, et al. (1999) Triggering cell death: The crystal structure of Apo2L/TRAIL in a complex with death receptor 5. *Mol Cell* 4(4):563–571.
16. Lin Y, Devin A, Rodriguez Y, Liu ZG (1999) Cleavage of the death domain kinase RIP by caspase-8 prompts TNF-induced apoptosis. *Genes Dev* 13(19):2514–2526.
17. Micheau O, Tschopp J (2003) Induction of TNF receptor I-mediated apoptosis via two sequential signaling complexes. *Cell* 114(2):181–190.
18. Kauppila S, et al. (2003) Eiger and its receptor, Wengen, comprise a TNF-like system in Drosophila. *Oncogene* 22(31):4860–4867.
19. Moreno E, Yan M, Basler K (2002) Evolution of TNF signaling mechanisms: JNK-dependent apoptosis triggered by Eiger, the Drosophila homolog of the TNF superfamily. *Curr Biol* 12(14):1263–1268.
20. Collette Y, Gilles A, Pontarotti P, Olive D (2003) A co-evolution perspective of the TNFSF and TNFRSF families in the immune system. *Trends Immunol* 24(7):387–394.
21. Wiens GD, Glenney GW (2011) Origin and evolution of TNF and TNF receptor superfamilies. *Dev Comp Immunol* 35(12):1324–1335.
22. Robertson AJ, et al. (2006) The genomic underpinnings of apoptosis in Strongylocentrotus purpuratus. *Dev Biol* 300(1):321–334.
23. Pandolfi JM, et al. (2003) Global trajectories of the long-term decline of coral reef ecosystems. *Science* 301(5635):955–958.
24. Hajnóczky G, Davies E, Madesh M (2003) Calcium signaling and apoptosis. *Biochem Biophys Res Commun* 304(3):445–454.
25. Freeman ME, Kanyicska B, Lerant A, Nagy G (2000) Prolactin: Structure, function, and regulation of secretion. *Physiol Rev* 80(4):1523–1631.
26. Einhauer A, Jungbauer A (2001) The FLAGTM peptide, a versatile fusion tag for the purification of recombinant proteins. *J Biochem Bioph Meth* 49(1-3):455–465.
27. Sen CK, Sashwati R, Packer L (1999) Fas mediated apoptosis of human Jurkat T-cells: Intracellular events and potentiation by redox-active alpha-lipoic acid. *Cell Death Differ* 6(5):481–491.
28. Kusserow A, et al. (2005) Unexpected complexity of the Wnt gene family in a sea anemone. *Nature* 433(7022):156–160.
29. Desvignes T, Pontarotti P, Bobe J (2010) Nme gene family evolutionary history reveals pre-metazoan origins and high conservation between humans and the sea anemone, Nematostella vectensis. *PLoS ONE* 5(11):e15506.
30. Beschin A, et al. (1999) Convergent evolution of cytokines. *Nature* 400(6745):627–628.
31. Beschin A, Bilej M, Torreele E, De Baetselier P (2001) On the existence of cytokines in invertebrates. *Cell Mol Life Sci* 58(5-6):801–814.
32. Scapigliati G, Buonocore F, Mazzini M (2006) Biological activity of cytokines: An evolutionary perspective. *Curr Pharm Des* 12(24):3071–3081.
33. Valanne S, Wang JH, Rämet M (2011) The Drosophila Toll signaling pathway. *J Immunol* 186(2):649–656.
34. Dinarello CA (1996) Biologic basis for interleukin-1 in disease. *Blood* 87(6):2095–2147.
35. Tourneur L, Chiocchia G (2010) FADD: A regulator of life and death. *Trends Immunol* 31(7):260–269.
36. Lasi M, David CN, Böttger A (2010) Apoptosis in pre-Bilaterians: Hydra as a model. *Apoptosis* 15(3):269–278.
37. Koyanagi R, et al. (2013) MarinegenomicsDB: An integrated genome viewer for community-based annotation of genomes. *Zoolog Sci* 30(10):797–800.
38. Petrache I, et al. (2003) Caspase-dependent cleavage of myosin light chain kinase (MLCK) is involved in TNF-alpha-mediated bovine pulmonary endothelial cell apoptosis. *FASEB J* 17(3):407–416.
39. Anderson JC, Peck SC (2008) A simple and rapid technique for detecting protein phosphorylation using one-dimensional isoelectric focusing gels and immunoblot analysis. *Plant J* 55(5):881–885.
40. Jovine L, Darie CC, Litscher ES, Wassarman PM (2005) Zona pellucida domain proteins. *Annu Rev Biochem* 74:83–114.
41. Faber BM, Chegini N, Mahony MC, Coddington CC III (2001) Macrophage secretory products and sperm zona pellucida binding. *Obstet Gynecol* 98(4):668–673.
42. Pernice M, et al. (2011) Regulation of apoptotic mediators reveals dynamic responses to thermal stress in the reef building coral Acropora millepora. *PLoS ONE* 6(1):e16095.
43. Tchernov D, et al. (2011) Apoptosis and the selective survival of host animals following thermal bleaching in zooxanthellate corals. *Proc Natl Acad Sci USA* 108(24): 9905–9909.
44. Portune KJ, Voolstra CR, Medina M, Szmant AM (2010) Development and heat stress-induced transcriptomic changes during embryogenesis of the scleractinian coral Acropora palmata. *Mar Genomics* 3(1):51–62.
45. DeSalvo MK, et al. (2010) Coral host transcriptomic states are correlated with Symbiodinium genotypes. *Mol Ecol* 19(6):1174–1186.
46. Reyes-Bermudez A, et al. (2009) Gene expression microarray analysis encompassing metamorphosis and the onset of calcification in the scleractinian coral Montastraea faveolata. *Mar Genomics* 2(3-4):149–159.
47. Ganot P, et al. (2011) Adaptations to endosymbiosis in a cnidarian-dinoflagellate association: Differential gene expression and specific gene duplications. *PLoS Genet* 7(7):e1002187.
48. Aranda M, et al. (2011) Differential sensitivity of coral larvae to natural levels of ultraviolet radiation during the onset of larval competence. *Mol Ecol* 20(14):2955–2972.
49. Barshis DJ, et al. (2013) Genomic basis for coral resilience to climate change. *Proc Natl Acad Sci USA* 110(4):1387–1392.
50. Cserzö M, Wallin E, Simon I, von Heijne G, Elofsson A (1997) Prediction of transmembrane alpha-helices in prokaryotic membrane proteins: The dense alignment surface method. *Protein Eng* 10(6):673–676.
51. Hulo N, et al. (2006) The PROSITE database. *Nucleic Acids Res* 34(Database issue): D227–D230.
52. Derbyshire MK, Lanczycki CJ, Bryant SH, Marchler-Bauer A (2012) Annotation of functional sites with the Conserved Domain Database. *Database (Oxford)* 2012: bar058.
53. Helman Y, et al. (2008) Extracellular matrix production and calcium carbonate precipitation by coral cells in vitro. *Proc Natl Acad Sci USA* 105(1):54–58.
54. Reyes-Bermudez A, Miller DJ (2009) In vitro culture of cells derived from larvae of the staghorn coral Acropora millepora. *Coral Reefs* 28(4):859–864.

Supporting Information

Quistad et al. 10.1073/pnas.1405912111

SI Materials and Methods

Bioinformatic Analysis of the TNFRSF and TNFSF in *Acropora digitifera*. Coral TNF ligands and receptors were extracted from the *Acropora digitifera* genome using the Pfam search option of TNF and TNF receptor (TNFR)_c6, respectively. In addition BLASTp was performed with extracted coral TNFs against the predicted coral proteome. The DAS transmembrane prediction server (1), PROSITE database (2), and the Conserved Domain Database (3) were used to analyze the predicted proteins, whereas Geneious software was used for manual annotations and construction of phylogenetic trees (4). *Homo sapiens* caspase-3, *H. sapiens* TRAF1, *H. sapiens* Fas, and *H. sapiens* TNFα were downloaded from the National Center for Biotechnology Information, and phylogenetic trees were constructed using the Jukes-Cantor neighbor-joining method with no outgroups. Homology detection and structure prediction by hidden Markov model-hidden Markov model comparison was performed with AdTNF1/AdTNFR1 and two representatives of the human TNF receptor-ligand superfamilies (TNFSF/TNFRSF): CD40L/CD40 (GI: 4557433, 114053977) (5).

Human Antibody Arrays. *Acropora yongeii* coral nubbins were exposed to heat shock (HS), cold shock (CS), the known coral pathogen *Vibrio coralliilyticus* (V), and human TNFα (HuTNFα) or were untreated (C1 and C2). Expression levels of unknown coral proteins bound to specific human antibodies were analyzed on a GenePix 4000B (Axon Instruments), and relative protein expression was determined. Interestingly, an unknown coral protein bound to the Fas human antibody had a relative expression of ∼75%, 60%, 40%, 25%, and 65% in C1, C2, HS, CS, and V treatments, respectively, whereas HuTNFα resulted in a complete disappearance of the protein (Fig. S3*A*). In addition, the human antibody CD40 (also a member of the TNFRSF) was undetectable in C1, C2, HS, CS, and V; however, HuTNFα resulted in relatively high expression of an unknown coral protein bound to the human CD40 antibody (Fig. S3*B*). Finally, a coral protein bound to the human Bcl-X_L antibody maintained expression levels >95% in all treatments; however, following HuTNFα stimulation, the expression of this coral protein was down-regulated by ∼97% (Fig. S3*C*). HuTNFα also affected the expression of unknown coral proteins bound to the antibodies of human proteins involved with mitochondrial protection, DNA damage response, cystoskeletal structure, and various CD receptors (Fig. S4 *A*–*O*). The HS and CS corals were maintained for a period of 3 h at 32 °C (6 °C above ambient) and 20 °C (6 °C below ambient), respectively, in a 2-L beaker with aeration. For the bacterial treatment, *V. coralliilyticus* was grown to a lawn on thiosulfate-citrate-bile salts-sucrose agar, scraped from the plate, and resuspended into 1 mL of seawater. Two hundred microliters of this suspension was injected directly into the tissue of the coral with a 25-gauge needle. For the HuTNFα treatment, HuTNFα was added to the seawater at a final concentration of 1 pg/mL and incubated for 2 h. To normalize for total protein added to the arrays, individual protein hits were ranked by total fluorescence above background level.

2D Gel Electrophoresis of *A. yongeii* Stimulated with HuTNFα. Aquaria-maintained *A. yongeii* was fragmented into two ∼6-cm "nubbins" and allowed to recover for 24 h. Each fragment was placed into 100 mL of seawater. One fragment was incubated with HuTNFα (H8916; Sigma-Aldrich) for 30 min at a final concentration of 1 pg/mL, whereas the second nubbin was incubated with no additional treatment as a control. Coral nubbins were airbrushed with 0.22-μm-filtered seawater (FSW) to remove the tissue from the skeleton, and protease inhibitor mixture (P2714; Sigma-Aldrich) was added to the blastate for a final concentration of 1×. Protein was then extracted as described by ref. 6, resuspended in 7 M urea, 2 M thiourea, 30 mM Tris, and 4% (vol/vol) CHAPS buffer (Cell Signal) and stored at −80 °C. 2D gel electrophoresis was performed, and significantly different spots between the treatment and control were selected for LC-MS (Aberdeen Proteomics and Samespots Software). Mass spectra data were searched against a custom-built *A. digitifera* database based on the predicted proteome (7).

Production of Crude AdTNF1 Using a Prolactin Secretion Scaffold. A DNA sequence containing AdTNF1 flanked by BamHI and XhoI restriction sites was obtained (DNA 2.0) and digested with BamHI and XhoI (Fermentas), and the extracted fragment was ligated into the retroviral vector pBMN.i.mCherry containing a psi promoter (stable expression), Kozak sequence (translational start site), and Prolactin signal sequence (protein secretion) (8), upstream of AdTNF1 (pBMN.i.mChAdTNF1). This vector was transformed into *Escherichia coli* XL-1 Blue amplified, and the ligated sequence was confirmed by primer extension sequencing (Eton Bioscience). A control vector containing GFP in place of AdTNF1 was also created (pBMN.i.mChGFP). Three micrograms of both vectors was separately transfected into 293T cells (ATCC) by mixing the plasmids with 125 μL of FCS-free DMEM and 30 μg of polyethylenimine (linear, MW 24000; Polysciences). Cells were maintained for 48 h in DMEM media supplemented with 10% (vol/vol) FBS (Gemini Bio-Products), penicillin G (100 U/mL), glutamine (2 mM), and streptomycin (100 μg/mL). Culture media from pBMN.i.mChAdTNF1- and pBMN.i.mChGFP-transfected cells were collected and used for further experimentation.

Direct Stimulation of Coral Cells with HuTNFα and Crude AdTNF1. To initiate coral cell cultures, methods were adapted from Helman et al. (9). Briefly, coral fragments were treated with calcium-free seawater supplemented with 3% (vol/vol) antibiotic-antimyotic solution (GIBCO) for 2.5 h with gentle shaking, followed by 30-min incubation in 0.22-μm FSW and 25 mM Hepes buffer supplemented with collagenase (Sigma-Aldrich) at a final concentration of 1.5 mg/mL. Fragments were then incubated overnight in cell culture media. Coral tissue was passed through a custom build 20-μm nylon cell strainer, washed three times with 0.22-μm FSW, and resuspended in 3 mL of culture media in a six-well cell culture plate. Cells were maintained under 12-h light/dark for 1 wk, followed by trypsinization (Cellgro). After 48 h, an individual ∼20-μm coral cell was identified and monitored in real time with confocal microscopy following HuTNFα exposure at final concentration of 1 pg/mL.

A second method adapted from ref. 10 was used to obtain a different coral cell type. *A. yongeii* nubbins were treated with three 15-min incubations in a 0.22-μm FSW solution containing ampicillin (270 μg/mL), streptomycin (135 μg/mL), and chloramphenicol (27 μg/mL) (Invitrogen). Corals were then submerged in cell culture media (9) in a 50-mL Falcon tube that was wrapped in aluminum foil for 48 h. Fifty microliters of sloughed-off coral tissue was resupsended into 1 mL of seawater, and 100 μL of coral cell solution was placed onto a glass slide within a humidified chamber. Cells were allowed to settle for 30 min before direct stimulation with HuTNFα at a final concentration of 1 pg/mL for 90 min, fixation with 2% (vol/vol) paraformaldehyde,

and staining with DAPI (10 μg/mL). Slides were then visualized on a flourescent microscope (Zeiss Axioplans Imaging). Visual apoptotic cell counts were corroborated with a Live/Dead Cell Stain Imaging Kit (Life Technologies) of coral cells exposed to HuTNFα for 4 h. For AdTNF1 stimulation, 10 μL of media from 293T cells tranfected with either pBMN.i.mChAdTNF1 or pBMN.i.mChGFP was added to 100 μL of resuspended coral cells.

Immunohistochemistry of Coral Cells Exposed to HuTNFα and Crude AdTNF1-FLAG. The FLAG epitope (DYKDDDDK) was cloned into the C terminus of AdTNF1 and confirmed with primer extension sequencing. AdTNF1-FLAG was then cloned into the Prolactin signal sequence secretion scaffold and transfected into 293T cells, and media were collected for further experimentation as described above. To obtain coral cells, adult coral tissue was incubated for 24 h under dark conditions in cell media (10) and centrifuged for 15 min at 4 °C and 1,500 × *g*. Cells were washed twice in ice cold PBS, resuspended in 1 mL of seawater, and aliqouted for further incubations. Cells were then treated with either HuTNFα, 200 μL of cell media from AdTNF1-FLAG-transfected cells, or left untreated on ice for 45 min and fixed in 2% (vol/vol) paraformaldehyde. Following fixation cells were washed twice in ice cold PBS and stained with either FLAG antibody (Sigma) or HuTNFα (R&D Systems) antibody, followed by further washes in PBS and staining with a FITC mouse secondary antibody (Sigma). Cells were then visualized on a flourescent microscope (Zeiss Axioplans Imaging).

Caspase Activity of Coral Cells Exposed to HuTNFα. Coral cells were isolated as described above (10) and allowed to equilibrate for 48 h. Cells were treated with a negative control inhibitor for caspase Z-FA-FMK (BD Pharmigen), negative control inhibitor, and HuTNFα, or the pan-caspase inhibitor Z-VAD-FMK (BD Pharmigen) and HuTNFα. Caspase assays were performed at 31 °C, and activity was quantified based on the linear slope of enzyme activity.

Flow Cytometric Analysis of Coral Bleaching. For HuTNFα stimulation, ∼4-cm coral nubbins from the same parent colony were fragmented and placed into separate 15-mL Falcon tubes containing 6 mL of seawater ± 80 pg/mL, and 400 μL of surrounding seawater was sampled for expelled algal cells, every 2 h for 12 h total. For AdTNF1 stimulation, six coral nubbins were fragmented into ∼2-cm pieces and randomly placed into six separate 15-mL Falcon tubes containing 10 mL of 0.2-μm FSW also supplemented with ampicillin (final concentration, 100 μg/mL). Three of the coral nubbins were treated with 200 μL of media from 293T cells transfected with pBMN.i.mChAdTNF1, whereas the other three were treated with cell media from untransfected cells. Surrounding seawater was sampled every 2 h for 12 h total. To enumerate concentrations of algae by flow cytometry, a 96-well plate containing 200 μL of each sample was loaded onto a BDFACSCanto (BD Biosciences) with a high-throughput sampler (HTS). A 100-μL aliquot was mixed three times by syringe and run using the HTS at 3 μL/s. Between each sample, the probe was rinsed with 400 μL of sheath to minimize carryover of samples. To quantify Zooxanthellae, a 633-nm laser line and a 660/20-nm band-pass filter were used. Additionally, a 488-nm laser line and a 530/30-nm band-pass filter was used to quantify the number of coral cells in the samples. During acquisition, the threshold was set to 200 for green (530/30BP) fluorescence OR 1,000 for red (660/20BP). After acquisition, data were exported as FCS3.0 and analyzed with FlowJo 7.6.3 (Treestar).

Flow Cytometric Analysis of Jurkat Cell Viability. To quantify cell viability, propidium iodide (PI) staining was performed and analyzed by flow cytometry in a 96-well plate format using BDFACSCanto [2 laser (4-2 color); BD Biosciences]. Cells were seeded at 6×10^6cells/mL in a final volume of 150 μL and grown for 48 h under various treatment conditions. PI was added to each well at a final concentration of 1×, which was excited by the blue (488 nm) laser and analyzed in the PerCP-Cy5.5 channel (670-nm long-pass filter preceded by a 655-nm long-pass filter). Using an HTS, 30-μL aliquots were mixed three times by the syringe and run at a flow rate of 2 μL/s. Between each sample, 800 μL of sheath fluid was used to rinse the syringe to ensure minimal carryover from sample to sample. During acquisition, the threshold was set at forward scatter 5,000, and 1×10^5 cells were recorded. After acquisition, the data were exported as FCS3.0 and analyzed with FlowJo 7.6.3 (Treestar).

1. Cserzö M, Wallin E, Simon I, von Heijne G, Elofsson A (1997) Prediction of transmembrane alpha-helices in prokaryotic membrane proteins: The dense alignment surface method. *Protein Eng* 10(6):673–676.
2. Hulo N, et al. (2006) The PROSITE database. *Nucleic Acids Res* 34(Database issue): D227–D230.
3. Derbyshire MK, Lanczycki CJ, Bryant SH, Marchler-Bauer A (2012) Annotation of functional sites with the Conserved Domain Database. *Database (Oxford)* 2012: bar058.
4. Drummond AJ, et al. (2010) Geneious v5.3 (Biomatters). Available at www.geneious.com. Accessed May 21, 2014.
5. Biegert A, Mayer C, Remmert M, Söding J, Lupas AN (2006) The MPI Bioinformatics Toolkit for protein sequence analysis. *Nucleic Acids Res* 34(Web Server issue):W335-9.
6. Bromage E, Carpenter L, Kaattari S, Patterson M (2009) Quantification of coral heat shock proteins from individual coral polyps. *Mar Ecol Prog Ser* 376:123–132.
7. Shinzato C, et al. (2011) Using the Acropora digitifera genome to understand coral responses to environmental change. *Nature* 476(7360):320–323.
8. Freeman ME, Kanyicska B, Lerant A, Nagy G (2000) Prolactin: structure, function, and regulation of secretion. *Physiol Rev* 80(4):1523–1631.
9. Helman Y, et al. (2008) Extracellular matrix production and calcium carbonate precipitation by coral cells in vitro. *Proc Natl Acad Sci USA* 105(1):54–58.
10. Reyes-Bermudez A, Miller DJ (2009) In vitro culture of cells derived from larvae of the staghorn coral Acropora millepora. *Coral Reefs* 28(4):859–864.

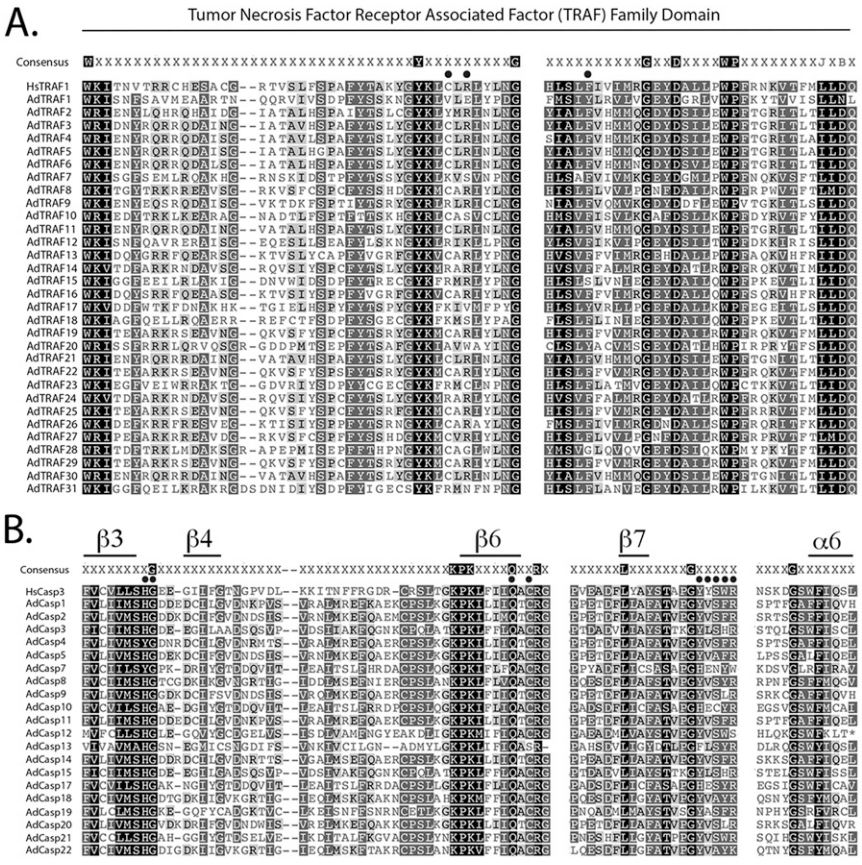

Fig. S1. Primary sequence alignments of *A. digitifera* and *H. sapiens* death receptor pathway proteins. (*A*) Primary sequence alignment of putative *A. digitifera* TNF receptor-associated factors (TRAFs) with *H. sapiens* TRAF1. (*B*) Primary sequence alignment of putative *A. digitifera* caspases with *H. sapiens* caspase-3. Amino acids conferring α- and β-secondary structures of *H. sapiens* caspase-3 are indicated by solid black lines, whereas side chains located in the active sites of *H. sapiens* caspase-3 are indicated by black dots.

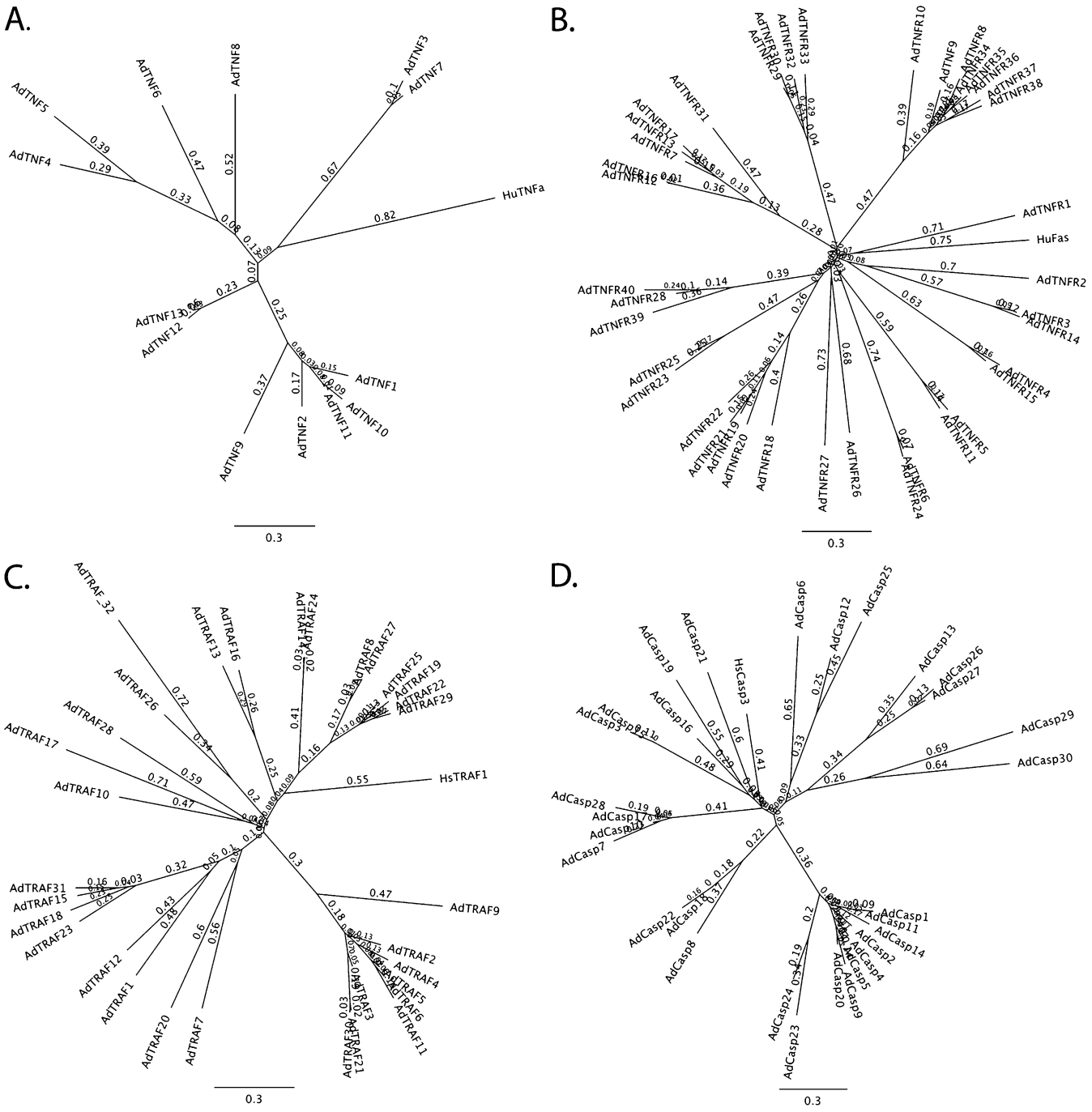

Fig. S2. Phylogenetic trees of *A. digitifera* and *H. sapiens* death receptor pathway proteins. (*A*) Phylogenetic tree of the *A. digitifera* TNF repertoire and HuTNFα with branches values indicating the number of substitutions per site. (*B*) Phylogenetic tree of *A. digitifera* TNF receptor repertoire and *H. sapiens* Fas with branch values indicating the number of substitutions per site. (*C*) Phylogenetic tree of *A. digitifera* TRAF repertoire and *H. sapiens* TRAF1 with branches values indicating the number of substitutions per site. (*D*) Phylogenetic tree of *A. digitifera* caspase repertoire and *H. sapiens* caspase-3 with branches values indicating the number of substitutions per site.

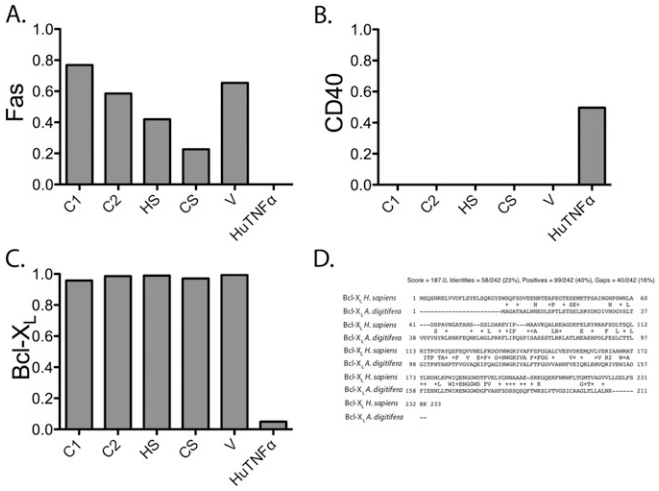

Fig. S3. HuTNFα affects the expression of unknown coral proteins bound to human antibodies involved with death receptor signaling. The expression of coral proteins bound to human Fas (*A*), CD40 (*B*), and Bcl-X_L (*C*) antibodies. (*D*) Primary sequence alignment of an *A. digitifera* Bcl-X_L-like protein with *H. sapiens* Bcl-X_L.

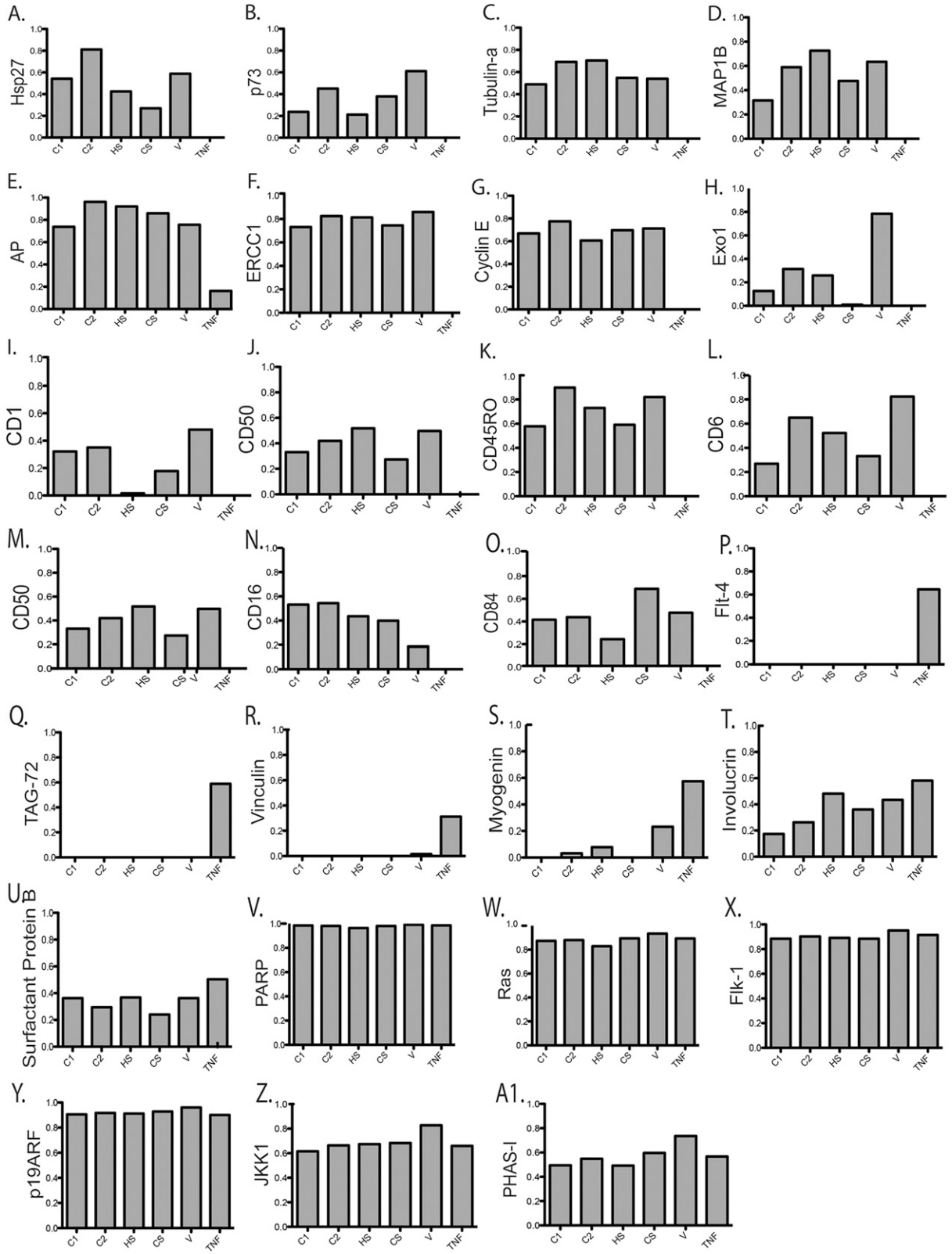

Fig. S4. Proteomic analysis of coral exposed to HuTNFα using human antibody arrays. Relative expression of coral proteins bound to various human antibodies from all six treatments. Human antibodies to antiapoptotic proteins (*A* and *B*) and cytoskeletal proteins (*C* and *D*) and involved with apoptotic signaling (*E–H*), CD proteins (*I–O*), up-regulated proteins (*P–T*), and stably expressed proteins (*U–A1*).

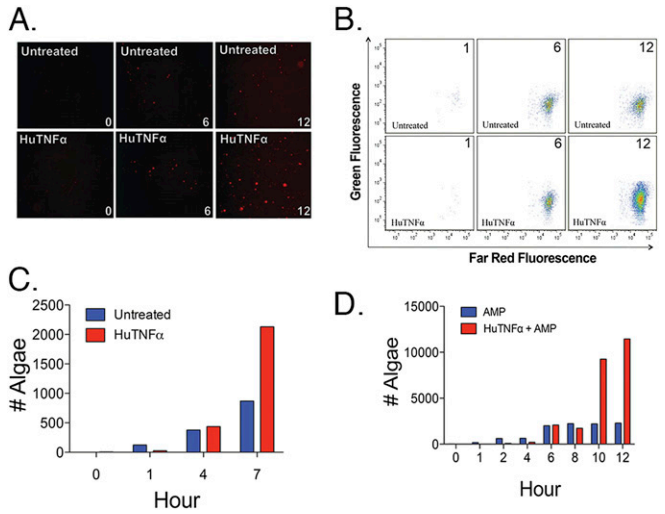

Fig. S5. The effect of HuTNFα on coral bleaching. (*A*) Representative images of expelled zooxanthallae at 0, 6, and 12 h of untreated (*Upper*) and HuTNFα-treated (*Lower*) coral. Red = zooxanthallae autofluorescence. (*B*) Total number of expelled zooxanthallae at 1, 6, and 12 h. (*C*) Total number of algae expelled from coral in untreated and HuTNFα exposure. (*D*) Total number algae expelled from coral exposed to ampicillin (AMP) and HuTNFα + AMP.

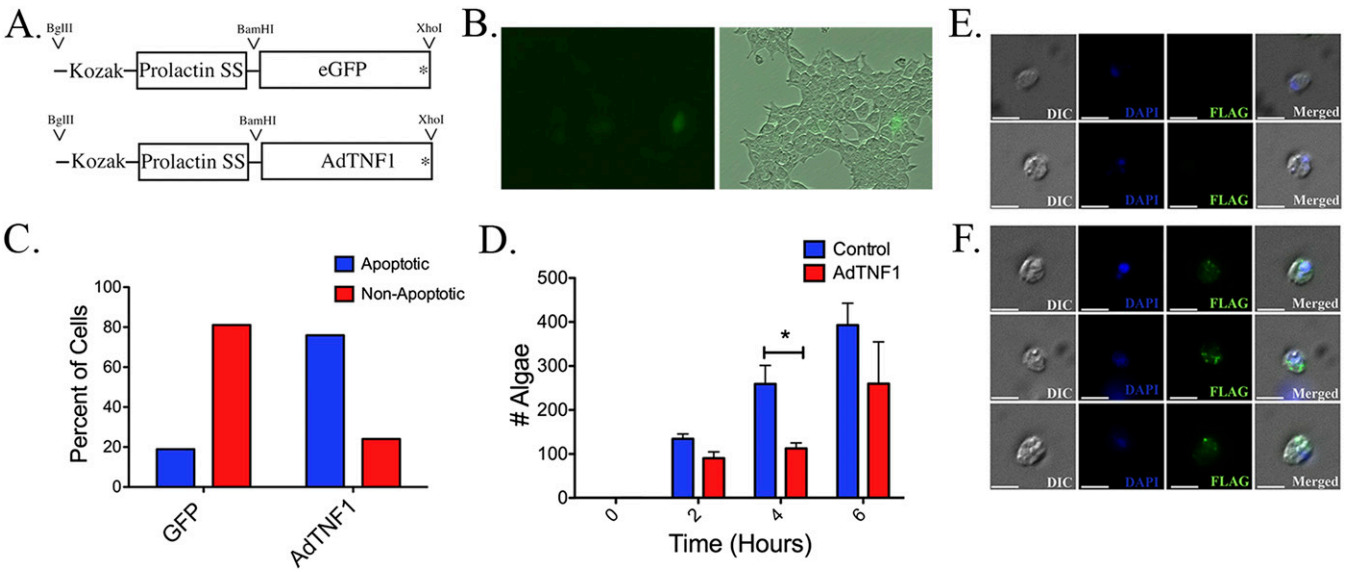

Fig. S6. The physiological and cellular responses of coral to crude AdTNF1. (*A*) Scaffold inserted into pBMN.i.mCh with Kozak sequence and Prolactin signal sequence. Secreted GFP (pBMN.i.mChGFP) and AdTNF1 (pBMN.i.mChAdTNF1). (*B*) Merged image of 293T cells transfected with pBMN.i.mChGFP under stable expression of GFP. (*C*) Percent of apoptotic cells following exposure to media from pBMN.i.mChAdTNF1-transfected 293T cells and secreted GFP (pBMN.i.mChGFP) ($n = 200$). (*D*) Total number of algae expelled from coral in media control ($n = 3$) and AdTNF1 exposed ($n = 3$), $^*P = 0.0295$; unpaired t test. (*E*) Representative coral cells incubated with FLAG antibody and stained with DAPI. (White bar, 5 μm.) (*F*) Representative coral cells incubated with AdTNF1-FLAG and FLAG antibody, stained with DAPI. (White bar, 5 μm.)

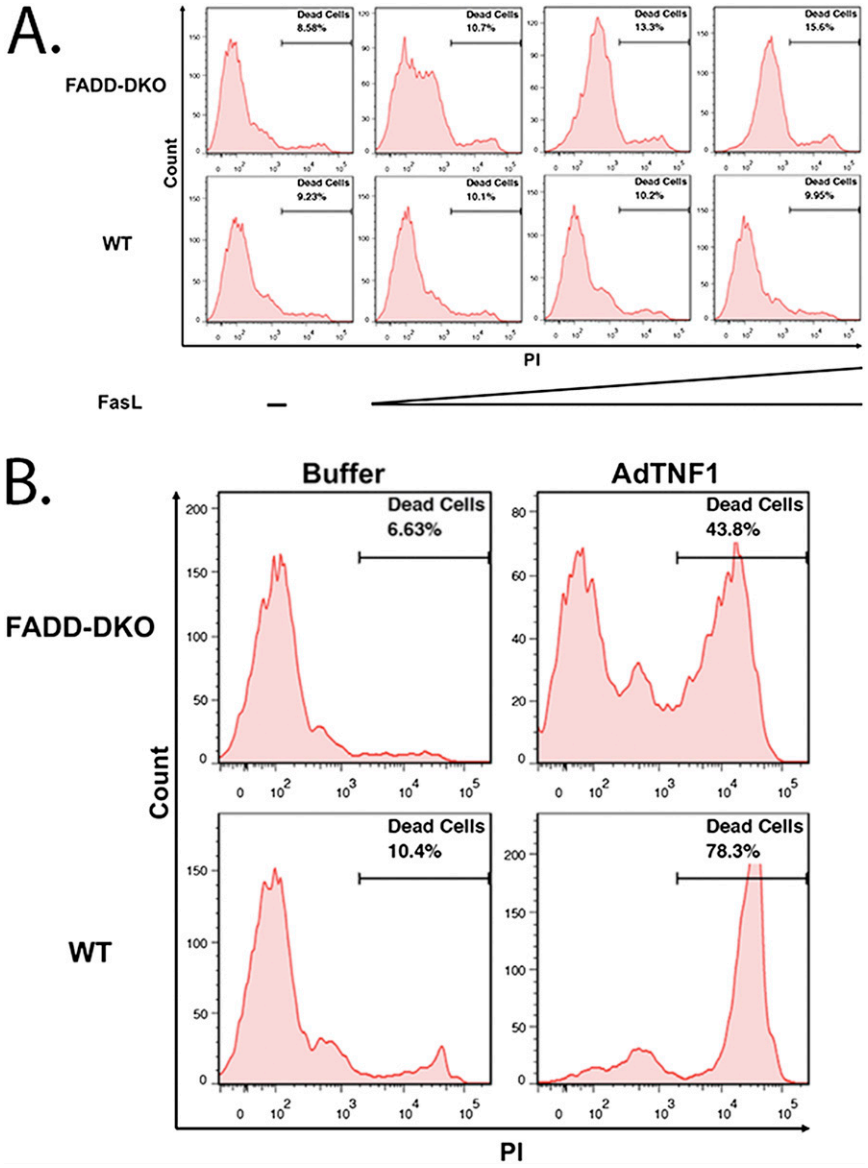

Fig. S7. Live/dead assay of Jurkat cells in the presence of FasL and purified AdTNF1. (*A*) Dose-dependent response of WT Jurkat cells to Fas ligand (*Upper*) and lack of cellular response of Fas-associated death domain protein (FADD) KO cells to FasL (*Lower*). (*B*) FADD-DKO Jurkat cells (*Upper*) and WT Jurkat cells (*Lower*) incubated for 48 h in buffer only (*Left*) and AdTNF1 (*Right*) shows a significant decrease in percent death of the death receptor knockdown cell line compared with the WT when analyzed.

Table S1. Bioinformatic characterization of putative *A. digitifera* TRAFS and caspases

Protein ID	Protein name	Length (amino acids)	Domain	Domain ID	E-value
aug_v2a.20266.t	AdTRAF1	721	MATH_TRAF_C	cd00270	3.61E-48
			RING	cd00162	6.56E-04
			MATH	cl02446	4.48E-32
			zf-TRAF	cl08341	9.82E-09
			zf-TRAF	cl08341	5.38E-08
			zf-TRAF	cl08341	3.71E-06
aug_v2a.21707.t1	AdTRAF2	521	MATH_TRAF_C	cd00270	1.40E-57
			RING	cd00162	4.79E-06
			zf-TRAF	cl08341	2.28E-10
			zf-TRAF	cl08341	1.08E-09
aug_v2a.21711.t1	AdTRAF3	466	MATH_TRAF_C	cd00270	9.92E-71
			zf-TRAF	cl08341	4.72E-13
			zf-TRAF	cl08341	1.15E-10
aug_v2a.22479.t1	AdTRAF4	264	MATH_TRAF_C	cd00270	3.77E-61
		392	RING	cd00162	2.77E-07
			MATH	cl02446	8.06E-39
			zf-TRAF	cl08341	4.36E-04
			zf-TRAF	cl08341	2.46E-03
aug_v2a.05503.t1	AdTRAF5	307	MATH_TRAF_C	cd00270	1.87E-68
			zf-TRAF	cl08341	7.30E-04
aug_v2a.00824.t2	AdTRAF6	352	MATH_TRAF_C	cd00270	2.37E-71
			zf-TRAF	cl08341	1.07E-03
aug_v2a.10503.t1	AdTRAF7		MATH_TRAF_C	cd00270	1.20E-59
			chaperonin	pf0118	0.00E+00
aug_v2a.12601.t1	AdTRAF8	277	MATH_TRAF_C	cd00270	3.52E-56
aug_v2a.01740.t1	AdTRAF9	272	MATH_TRAF_C	cd00270	2.90E-49
			HemX	cl19375	2.16E-03
aug_v2a.16435.t1	AdTRAF10	384	MATH_TRAF_C	cd00270	1.81E-63
			zf-TRAF	cl08341	1.83E-11
			zf-TRAF	cl08341	1.16E-04
aug_v2a.18053.t1	AdTRAF11	1250	MATH_TRAF_C	cd00270	3.99E-68
			zf-TRAF	cl08341	1.68E-13
			zf-TRAF	cl08341	8.83E-05
aug_v2a.20009.t1	AdTRAF12	391	RING	cd00162	8.09E-03
			MATH	cl02446	1.70E-37
			zf-TRAF	cl08341	1.12E-11
			zf-TRAF	cl08341	7.76E-07
aug_v2a.20535.t1	AdTRAF13	531	MATH	cl02446	1.68E-79
			zf-TRAF	cl08341	2.43E-10
			zf-TRAF	cl08341	4.19E-04
			FliJ	pfam02050	3.78E-03
aug_v2a.20539.t1	AdTRAF14	541	RING	cd00162	4.52E-05
			MATH	cl02446	4.54E-76
			zf-TRAF	cl08341	1.85E-04
			zf-TRAF	cl08341	2.50E-03
aug_v2a.04463.t1	AdTRAF15	380	RING	cd00162	2.37E-06
			MATH	cl02446	2.60E-36
			zf-TRAF	cl08341	6.47E-11
			zf-TRAF	cl08341	1.04E-03
aug_v2a.23514.t	AdTRAF16	556	RING	cd00162	4.48E-06
			MATH	cl02446	2.24E-87
			zf-TRAF	cl08341	2.04E-09
			zf-TRAF	cl08341	9.04E-06
			FliJ	pfam02050	9.93E-03
aug_v2a.05655.t1	AdTRAF17	574	RING	cd00162	8.89E-03
			MATH	cl02446	7.03E-69
			zf-TRAF	cl08341	6.88E-12
			zf-TRAF	cl08341	1.75E-05
aug_v2a.06167.t1	AdTRAF18	437	RING	cd00162	4.17E-06
			MATH	cl02446	1.30E-34
			zf-TRAF	cl08341	5.53E-05
aug_v2a.06787.t1	AdTRAF19	469	RING	cd00162	1.42E-03
			MATH	cl02446	2.30E-81

Table S1. Cont.

Protein ID	Protein name	Length (amino acids)	Domain	Domain ID	E-value
aug_v2a.06805.t2	AdTRAF20	379	MATH	cl02446	6.39E-38
			zf-TRAF	cl08341	1.46E-14
aug_v2a.11189.t4	AdTRAF21	343	MATH	cl02446	3.97E-67
			zf-TRAF	cl08341	3.90E-10
aug_v2a.13867.t1	AdTRAF22	494	MATH	cl02446	1.30E-84
			zf-TRAF	cl08341	1.70E-04
			zf-TRAF	cl08341	1.19E-03
aug_v2a.15460.t1	AdTRAF23	432	MATH	cl02446	1.45E-40
			zf-TRAF	cl08341	3.81E-11
aug_v2a.16670.t1	AdTRAF24	538	RING	cd00162	1.95E-04
			MATH	cl02446	4.22E-76
			zf-TRAF	cl08341	1.87E-04
			zf-TRAF	cl08341	4.13E-03
aug_v2a.17026.t1	AdTRAF25	420	MATH	cl02446	4.16E-79
			zf-C3HC4_2	pfam13923	3.39E-03
aug_v2a.17660.t1	AdTRAF26	526	MATH	cl02446	1.04E-83
			zf-TRAF	cl08341	1.60E-13
			zf-TRAF	cl08341	1.94E-04
aug_v2a.18329.t1	AdTRAF27	455	MATH	cl02446	8.46E-57
			zf-TRAF	cl08341	1.88E-04
			zf-RING_5	pfam14634	9.72E-03
aug_v2a.10543.t1	AdTRAF28	296	zf-TRAF	cl08341	2.00E-09
			MATH	cl02446	5.72E-33
aug_v2a.13869.t1	AdTRAF29	568	MATH	cl02446	1.15E-83
			zf-TRAF	cl08341	1.90E-03
			zf-TRAF	cl08341	4.85E-03
aug_v2a.11189.t1	AdTRAF30	463	RING	cd00162	4.21E-07
			MATH	cl02446	1.84E-65
			Zinc_peptidase	cl14876	1.98E-46
			zf-TRAF	cl08341	3.42E-09
			U-box	cl17544	6.94E-03
aug_v2a.15461.t1	AdTRAF31	420	RING	cd00162	3.67E-09
			MATH	cl02446	3.22E-35
			zf-TRAF	cl08341	1.67E-03
aug_v2a.01920.t1	AdTRAF32	232	MATH	cl02446	2.17E-48
			BTB	pfam00651	1.43E-28
aug_v2a.00817.t2	AdCasp1	574	CASc	cl00042	6.57E-52
			CASc	cl00042	2.16E-25
aug_v2a.04862.t1	AdCasp2	565	CASc	cd00032	9.23E-68
			CASc	cl00042	6.15E-31
aug_v2a.05413.t1	AdCasp3	343	CASc	cd00032	2.03E-67
aug_v2a.10482.t1	AdCasp4	1561	CASc	cd00032	5.00E-64
			CASc	cl00042	2.28E-59
			CASc	cl00042	2.79E-27
			CASc	cl00042	9.62E-22
			GT1_YqgM_like	cd03801	1.57E-18
			RfaG	COG0438	2.87E-18
aug_v2a.10962.t1	AdCasp5	678	CASc	cd00032	6.43E-65
			CASc	cl00042	1.04E-23
aug_v2a.11989.t1	AdCasp6	277	CASc	cl00042	2.35E-46
aug_v2a.14264.t1	AdCasp7	555	CASc	cl00042	5.08E-57
aug_v2a.15985.t1	AdCasp8	475	CASc	cd00032	8.74E-67
aug_v2a.17260.t1	AdCasp9	936	CASc	cl00042	5.97E-50
			CASc	cl00042	5.04E-28
			GT1_YqgM_like	cd03801	6.03E-27
			RfaG	COG0438	3.52E-25
aug_v2a.19602.t1	AdCasp10	260	CASc	cd00032	9.06E-81
	AdCasp11	472	CASc	cd00032	5.93E-68
			CASc	cl00042	7.35E-29
aug_v2a.00023.t1	AdCasp12	362	CASc	cd00032	7.35E-71
			CARD	cd01671	5.98E-23
aug_v2a.01975.t1	AdCasp13	776	CASc	cd00032	1.78E-69

Table S1. Cont.

Protein ID	Protein name	Length (amino acids)	Domain	Domain ID	E-value
aug_v2a.00818.t1	AdCasp14	948	CASc	cd00032	2.18E-63
			CASc	cl00042	1.22E-34
aug_v2a.05412.t1	AdCasp15	205	CASc	cl00042	2.27E-60
aug_v2a.11988.t1	AdCasp16	114	CASc	cl00042	3.95E-40
aug_v2a.20139.t1	AdCasp17	181	CASc	cl00042	6.49E-67
aug_v2a.03841.t1	AdCasp18	237	CASc	cd00032	3.45E-70
aug_v2a.09611.t1	AdCasp19	431	CASc	cd00032	3.18E-86
			CARD	cd01671	1.38E-19
aug_v2a.10651.t1	AdCasp20	398	CASc	cl00042	5.91E-34
			CASc	cl00042	6.66E-24
aug_v2a.17832.t1	AdCasp21	492	CASc	cd00032	2.42E-79
			DED	cd00045	5.95E-23
			DED	cd00045	2.69E-22
aug_v2a.21759.t1	AdCasp22	384	CASc	cd00032	1.77E-67
aug_v2a.04318.t1	AdCasp23	669	CASc	cl00042	9.58E-26
aug_v2a.24718.t1	AdCasp24	531	CASc	cl00042	2.01E-25
			RT_like	cl02808	1.10E-08
			RT_like	cl02808	9.22E-05
			RVT_1	pfam0078	8.57E-12
aug_v2a.08731.t1	AdCasp25	570	Peptidase_C14	pfam00656	1.96E-20
			Ig super family	cl11960	1.33E-08
			Ig super family	cl11960	2.80E-03
			IGc2	smart00408	1.66E-06
			IG_like	smart00410	1.07E-03
aug_v2a.01506.t	AdCasp26	926	CASc	cd00032	4.53E-63
			DUF3733	pfam12534	5.38E-16
			LRR_4	pfam12799	3.38E-06
			DUF3733	cl13911	6.00E-04
			LRR_R	cd00116	6.88E-04
			LRR_8	pfam13855	1.34E-09
aug_v2a.01505.t1	AdCasp27	589	CASc	cd00032	6.65E-71
			DUF3733	pfam12534	1.16E-17
			DUF3733	cl13911	5.59E-05
aug_v2a.17122.t1	AdCasp28	467	CASc	cd00032	8.46E-82
			Rab32_Rab38	cd04107	2.15E-80
			COG1100	COG1100	2.47E-30
aug_v2a.17251.t1	AdCasp29	369	Ig	cd00096	7.10E-11
			Peptidase_C14	pfam00656	1.06E-16
			DD super family	cl14633	7.87E-04
			IG_like	smart00410	5.93E-13
aug_v2a.17673.t1	AdCasp30	635	Peptidase_C14	pfam00656	1.87E-27
			DD super family	cl14633	7.50E-13

Table S2. Putative TNF ligand repertoire of *A. digitifera*

Genome ID	Protein	Length (amino acids)	TNFSF	TI (7)	TNFBD (6)	TMD
aug_v2a.02274.t1	AdTNF1	162	32–160	7	5	Y
aug_v2a.01701.t1	AdTNF2	177	47–175	7	5	Y
aug_v2a.15174.t1	AdTNF3	178	53–151	6	3	Y
aug_v2a.19174.t1	AdTNF4	302	156–282	7	5	Y
aug_v2a.19173.t1	AdTNF5	243	105–225	7	4	Y
aug_v2a.19172.t1	AdTNF6	489	376–484	6	3	Y
aug_v2a.21762.t1	AdTNF7	443	52–150	6	3	N
aug_v2a.24713.t1	AdTNF8	373	228–303	7	5	N
aug_v2a.21776.t1	AdTNF9	154	46–150	5	4	N
aug_v2a.17595.t1	AdTNF10	170	42–168	7	5	N
aug_v2a.14625.t1	AdTNF11	81	1–73	4	2	N
aug_v2a.06643.t1	AdTNF12	97	1–95	7	1	N
aug_v2a.01699.t1	AdTNF13	97	1–95	6	1	N

N, no; TI, trimer interface, number indicates amount of residues present out of 7; TMD, transmembrane domain presence; TNFSF, TNF superfamily; TNFBD, TNF binding domain, number indicates amount of residues present out of 6; Y, yes.

Table S3. Putative TNF receptor repertoire of *A. digitifera*

Protein	Genome ID	Length (amino acids)	DD	Ig	CRD	50s loop	90s loop
AdTNFR1	aug_v2a.12827.t1	315	1	0	4	2	1
AdTNFR2	aug_v2a.07010.t1	431	1	0	3	2	1
AdTNFR3	aug_v2a.11053.t1	369	1	0	3	2	1
AdTNFR4	aug_v2a.16749.t2	383	1	0	2	1	1
AdTNFR5	aug_v2a.14243.t1	447	1	0	1	1	1
AdTNFR6	aug_v2a.09680.t1	477	1	0	1	1	1
AdTNFR7	aug_v2a.07000.t1	626	1	0	1	1	1
AdTNFR8	aug_v2a.02522.t1	791	1	0	1	1	0
AdTNFR9	aug_v2a.06604.t1.2	482	1	0	1	1	0
AdTNFR10	aug_v2a.06605.t1	585	1	0	1	1	0
AdTNFR11	aug_v2a.09194.t1	334	1	0	0	1	1
AdTNFR12	aug_v2a.03207.t1	725	0	0	4	2	2
AdTNFR13	aug_v2a.06998.t1	581	0	0	3	2	2
AdTNFR14	aug_v2a.11053.t2	621	0	0	3	2	1
AdTNFR15	aug_v2a.14012.t1	373	0	0	3	1	1
AdTNFR16	aug_v2a.07238.t1	491	0	0	2	1	1
AdTNFR17	aug_v2a.23226.t1	873	0	0	2	1	1
AdTNFR18	aug_v2a.23749.t1	744	0	1	1	1	1
AdTNFR19	aug_v2a.23750.t1	625	0	1	1	1	1
AdTNFR20	aug_v2a.06081.t1	499	0	1	1	1	1
AdTNFR21	aug_v2a.09846.t1	566	0	1	1	1	1
AdTNFR22	aug_v2a.17562.t1	608	0	1	1	1	1
AdTNFR23	aug_v2a.14077.t1	440	0	0	1	1	1
AdTNFR24	aug_v2a.04396.t2	597	0	0	1	1	1
AdTNFR25	aug_v2a.14078.t1	285	0	0	1	1	1
AdTNFR26	aug_v2a.00712.t1	272	0	0	1	1	1
AdTNFR27	aug_v2a.14960.t1	409	0	0	1	1	1
AdTNFR28	aug_v2a.00714.t1	247	0	0	1	1	1
AdTNFR29	aug_v2a.07001.t1	295	0	0	1	1	1
AdTNFR30	aug_v2a.07408.t1	348	0	0	1	1	1
AdTNFR31	aug_v2a.16417.t1	411	0	0	1	1	1
AdTNFR32	aug_v2a.19022.t1	446	0	0	1	1	1
AdTNFR33	aug_v2a.17969.t1	422	0	0	1	1	1
AdTNFR34	aug_v2a.06604.t1.1	797	0	0	1	1	0
AdTNFR35	aug_v2a.18371.t2	775	0	0	1	1	0
AdTNFR36	aug_v2a.18783.t1	812	0	0	1	1	0
AdTNFR37	aug_v2a.18784.t1.1	453	0	0	1	1	0
AdTNFR38	aug_v2a.18784.t1.2	651	0	0	1	1	0
AdTNFR39	aug_v2a.08700.t1	335	0	0	0	1	1
AdTNFR40	aug_v2a.00715.t1	372	0	0	0	1	1

CRD, cysteine-rich domain; DD, death domain; Ig, Ig domain; 50s loop, TNF ligand binding site; 90s loop, TNF receptor oligimerization site.

Table S4. Previously identified TNF receptor/ligand family members across evolution

Phylum	Organism	TNFSF	TNFRSF (DD)
Cnidaria*	*A. digitifera*	14	40 (11)
Cnidaria	*N. vectensis*	6	14
Mollusk	Abalone/scallop	2	1 (1)
Arthropod	*D. melangastor*	1	1 (0)
Echinoderm	*S. purpatus*	4	7 (3)
Urochordate	Sea squirts	2	2 (1)
Telost	*D. rerio*	17	~33 (8)
Amphibian	*Xenopus*	13	>3 (3)
Avian	Gallus	10	11 (4)
Mammalia	*H. sapiens*	18	29 (8)

DD, number of TNF receptors that contain a death domain; TNFRSF, TNF receptor superfamily; TNFSF, TNF superfamily.
*This study.

Table S5. Proteins identified through MS with the best hit to either the *A. digitifera* or Symbiodinium proteome

Spot no.	Protein ID/GI	Domains present	Organism
1	adi_v1.07627	Zona_pellucida	Coral
2	adi_v1.18643	Myosin_Tail_1, Tropomysoin, Intermediate Filament	Coral
3	adi_v1.18643	Myosin_Tail_1, Tropomysoin, Intermediate Filament	Coral
4	adi_v1.04802	Zona_pellucida	Coral
4	adi_v1.04802	Zona_pellucida	Coral
4	adi_v1.04802	Zona_pellucida	Coral
5	adi_v1.18643	Myosin_Tail_1, Tropomysoin, Intermediate Filament	Coral
6	adi_v1.18643	Myosin_Tail_1, Tropomysoin, Intermediate Filament	Coral
7	adi_v1.16781	Calreticulin	Coral
8	384383661	Peridinin-chlorophyll a-binding protein	Zooxanthallae
9	adi_v1.02613	Asp_Glu_race	Coral
10	adi_v1.02613	Asp_Glu_race	Coral
11	adi_v1.04828	14–3-3	Coral
12	adi_v1.01410	AhpC-TSA, Redoxin, 1-cysPrx_C	Coral
13	adi_v1.23158	efhand	Coral
14	adi_v1.05155	14–3-3	Coral
15	adi_v1.14836	efhand	Coral
16	adi_v1.10342	E1_DerP2_DerF2	Coral